Analysis of neutral particle recycling and pedestal fueling in a H-mode DIII-D discharge

Z. W. Friis,[1] W. M. Stacey,[1,a)] A. W. Leonard,[2] and M. E. Rensink[3]
[1]*Georgia Institute of Technology, Atlanta, Georgia 30332, USA*
[2]*General Atomics, San Diego, California 92186, USA*
[3]*Lawrence Livermore National Lab, Livermore, California 94551, USA*

(Received 17 August 2009; accepted 8 January 2010; published online 23 February 2010)

A detailed analysis of neutral atom recycling and pedestal fueling in a DIII-D [J. Luxon, Nucl. Fusion **42**, 614 (2002)] high-confinement mode discharge is presented. Experimental data and two-dimensional (2D) edge plasma fluid code calculations are employed to provide ion wall recycling and recombination neutral sources and background edge plasma parameters for a 2D edge neutral code calculation of detailed neutral density, ionization, and charge-exchange distributions throughout the edge pedestal, scrape-off layer and surrounding halo region, divertor, and private flux regions. The effectiveness of the different neutral sources for fueling the confined plasma is evaluated. © *2010 American Institute of Physics*. [doi:10.1063/1.3305809]

I. INTRODUCTION

The recycling of neutral atoms in the plasma edge is an area of increasing interest in tokamak plasma physics. Early experimental studies of neutral particle dynamics[1] and penetration into the core plasma[2] stimulated investigations of the effects of neutrals upon edge phenomena such as multifaceted axisymmetric radiation from the edge (MARFEs[3,4]), the low-to-high (L-H) mode transition,[5–7] the structure of the edge pedestal[8,9] in H-mode plasmas, and the interpretation of thermal transport coefficients from measurements of edge density and temperature gradients.[10]

Recent studies have focused on the investigation of edge pedestal fueling by neutrals produced from ions recycling from edge plasma material surfaces. At issue is whether the edge pedestal is fueled primarily by neutrals recycling from ion fluxes incident on the divertor target plates, as has long been assumed, or by neutrals recycling from the main plasma chamber wall produced by radial convective ion fluxes in the scrape-off layer (SOL). Evidence for both divertor recycling[11,12] and main chamber recycling[13–15] stimulated an extensive data collection, analysis, and modeling effort for a series of DIII-D discharges,[16] which concluded that divertor recycling was the primary fueling mechanism in DIII-D.

Our purpose in this paper is to make use of this extensive data compilation/analysis and background plasma calculation database that has been established for this series of DIII-D discharges for a detailed analysis of neutral particle recycling and edge pedestal fueling in a H-mode tokamak plasma with the two-dimensional (2D) neutral particle transport code GTNEUT.[17,18] We chose the deterministic GTNEUT code instead of the more familiar Monte Carlo codes such as DEGAS2 (Ref. 19) and EIRENE (Ref. 20), which are frequently used with plasma fluid codes such as SOLPS (discussed in Ref. 21) and UEDGE (Ref. 22) for neutral recycling calculations in tokamak plasmas because of the difficulty of obtaining sufficiently good statistics to calculate accurate neutral profiles with Monte Carlo (see, e.g., Fig. 17 in Ref. 21). The ion flux measurements and the GTNEUT code are summarized in Secs. II and III, respectively. The neutral particle recycling and pedestal fueling calculations are discussed in Sec. IV. Analyses of the relative importance of neutrals recycled at different spatial locations and discussion of the calculational uncertainties are also presented in Sec. IV. Suggestions for improvements to the GTNEUT code are briefly discussed in Sec. V. A brief summary and conclusions are presented in Sec. VI.

II. DIII-D NEUTRAL PARTICLE RECYCLING MEASUREMENTS

In recent DIII-D analyses, Leonard *et al.*[13,16] developed techniques to experimentally determine ion fluxes to the wall. The principle technique used to find the ion flux to the divertor target plates was by integrating the ion saturation current profile over the surface mounted Langmuir probes along the divertor target. The location of the divertor Langmuir probes are depicted in Fig. 1(a).

Ion fluxes to the wall from main chamber recycling were inferred from a "window frame" analysis.[13] The window frame analysis utilizes data from the midplane insertable Langmuir probe, Thomson scattering, and the Langmuir probe near the upper baffle. The locations of these diagnostics and their respective outputs are depicted in Fig. 1(a). The window frame analysis determines a global ion flux to the outboard chamber. In Ref. 16, it was noted that low midplane probe currents suggested the ion flux was mainly to the baffles so that the recycling neutral source due to this ion flux is distributed evenly between the upper and lower baffles. A distribution of the ion current to the wall for both the divertor and baffle sources is presented later.

The 2D edge fluids code UEDGE,[22] which has been used extensively[6,8,11–13,16,23] to interpret DIII-D edge plasma phenomena, was used to determine the background edge plasma parameters. This determination and reconciliation with spec-

a)Electronic mail: weston.stacey@nre.gatech.edu.

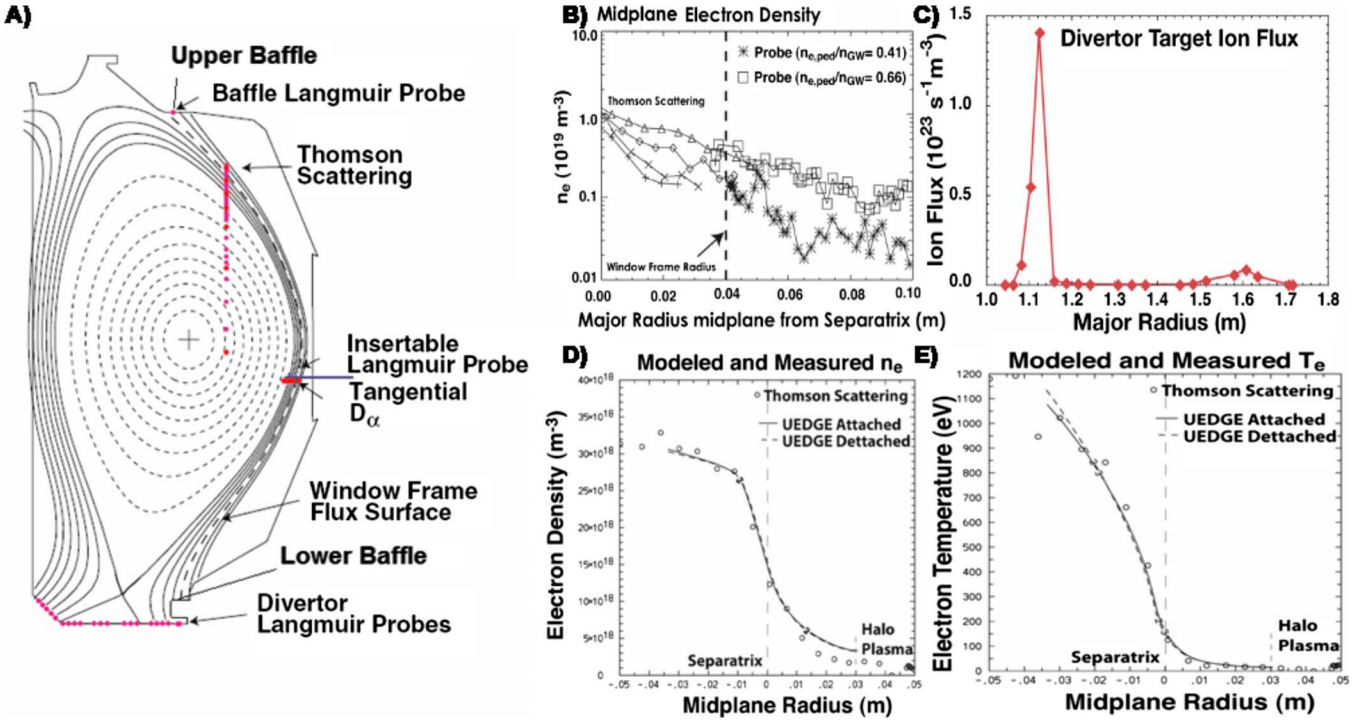

FIG. 1. (Color online) (a) DIII-D geometry showing the divertor configuration and the location where most of the main chamber ion flux recycles as well as where most of the divertor ion flux recycles. (b) Midplane probe data. (c) Divertor target ion flux ascertained from the surface mounted Langmuir probes along the strike plates. Thomson scattering data for (d) density and (e) temperature [(a) and (b) are reproduced with permission from Refs. 13 and 16].

troscopic data of the background plasma parameters are described in detail in earlier work.[11,13,16] The transport coefficients in the edge pedestal were adjusted to obtain agreement between calculated and measured densities and temperatures at the Thomson scattering diagnostic locations shown in Fig. 1(a), thus validating the calculated background by comparison with experiment in the edge pedestal. Figures 1(d) and 1(e) show that the UEDGE calculation matches well with the Thomson data.

There were no adequate experimental data in the divertor region to benchmark the UEDGE calculation to experimental data in this region.[16] Thus, two different sets of background plasma parameters were calculated[16] with UEDGE to bracket the actual experimental conditions (both benchmarked to the upstream Thomson data) by varying the wall recycling coefficients in UEDGE. Following these authors,[16] we denote these two calculated background plasmas as "attached" (high T) and "detached" (low T). In the attached case, the temperature near the inboard divertor plate is fairly high ($\sim$10 eV within a cm of the plate). In the detached case, the inboard divertor temperature is much lower ($\sim$1 eV within 1 cm of the plate). We emphasize that we are analyzing a single DIII-D discharge using two different sets of previously calculated background plasma parameters in order to bracket the likely divertor plasma parameters.

We further note that the GTNEUT neutrals calculation and the UEDGE background plasma calculations have not been iterated to consistency. The UEDGE background plasma calculations include an approximate fluid neutrals calculation and are adjusted to match the measured "upstream" plasma conditions in the outboard midplane (OUTMID) edge pedestal and SOL. Then, the more geometrically detailed GTNEUT calculations (extending the neutral transport to the plasma chamber wall) are carried out on a fixed background plasma to investigate in detail the neutral particle recycling and core refueling.

Because of the different ranges of temperatures and densities in the SOL, divertor, and pedestal regions, the neutral mean free paths (MFPs) can vary by large amounts, as shown in Fig. 2 for the detached plasma background, for which neutral MFPs range from less than 1 cm at the divertor plate to close to 60 m in the private flux region (PFR). In the attached case, the MFP lengths in the SOL-DIV region range from less than 1 cm to well over 30 m in the PFR.

The recombination rates calculated with UEDGE (Ref. 22) are quite different for the attached and detached background plasmas. In the attached case, the source of neutrals due to recombination is small (1.473×10^{20}/s in front of the inboard divertor plate); however, in the detached background plasma case, the temperatures are so low and the density is so high that the neutral atom source due to recombination becomes quite substantial (6.243×10^{21}/s in front of the inboard divertor plate) relative to the attached background plasma case.

The core ion particle source due to neutral beam injection for this discharge is known from experiment to be 3.86×10^{20}/s. Note that the neutral beam source is not included as a source in the neutrals calculations but as a source of ions.

Since the UEDGE code does not calculate the core plasma transport, the ion outflux must be determined from experiment. Using a method proposed by Porter,[23] the ion outflow

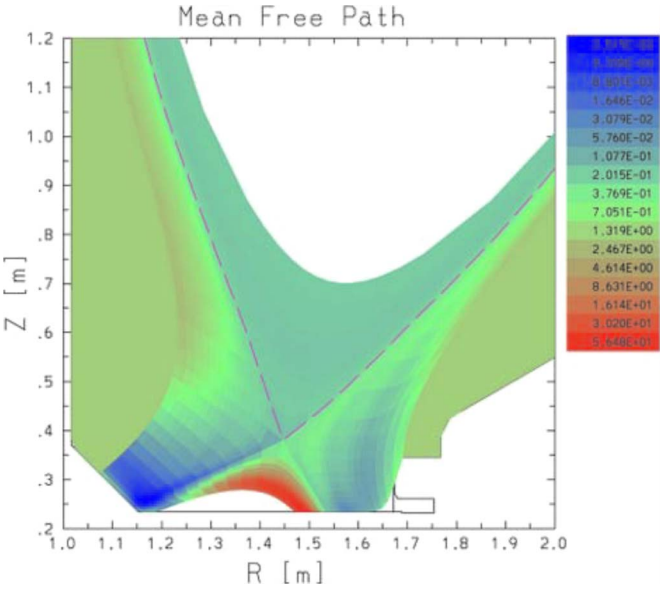

FIG. 2. (Color online) Neutral MFP distribution [UEDGE detached plasma background) calculated with the UEDGE code (Ref. 22)].

across the separatrix was estimated[16] from the density rise just after the L-H transition by assuming the separatrix ion flux was diffusive with a uniform diffusion coefficient equal to 25% of the effective heat diffusivity inferred from the experimental temperature gradient. This estimated ion outflux across the separatrix was 2.74×10^{21}/s, with an estimated uncertainty[23] of $\pm30\%$ due to experimental uncertainty. There are additional modeling uncertainties associated with assumptions such as a diffusive ion particle flux and a constant diffusion coefficient over the separatrix, which would increase this uncertainty in the ion outflux, but these cannot be readily estimated.

III. GTNEUT CODE

The GTNEUT code[17,18] is a 2D neutral particle transport code based on the transmission-escape probabilities (TEP) method[24,25,18] that is capable of accurately representing the complex geometry of the tokamak plasma edge and of providing an efficient calculation of neutral particle distributions and reaction rates. The GTNEUT code has been extensively benchmarked against Monte Carlo calculations and compared with experiments,[26–28,18] albeit for less detailed geometric models than are used in the analysis of this paper. Several refinements[18] of the TEP methodology (average neutral energy and DP1 transport approximation), not included in the original public release version of the GTNEUT code, are included in the version used for this paper.

In order to undertake the analysis presented in this paper, it was necessary to develop a methodology to construct a geometric computational grid from an equilibrium flux surface fit [EFIT (Ref. 29)] in order that background plasma parameters taken from experiment or calculated with 2D fluid plasma edge codes could be mapped to the GTNEUT computation grid. A new semiautomated method of grid generation was created[30] by adapting the UEDGE mesh generation routines.[22] The UEDGE mesh structure was extended to the walls of the confinement vessel in order to be able to treat wall recycling of neutral particles. Routines were also written to extract the background plasma parameters directly from UEDGE files. Thus, once a UEDGE problem has been run, it is straightforward to set up the corresponding GTNEUT problem.

The wall recycling model included in GTNEUT (Ref. 17) recycles incident ions or neutrals as either atoms (at a fraction of the average incident energy) or as molecules, with coefficients that depend on the incident energy and wall material. The molecules are assumed to be dissociated in the first grid region in front of the wall (with reference to Fig. 3, the HALO region in the main chamber, and the first grid regions in front of the divertor plates) into atoms at the Franck–Condon energy, which are transported with a corresponding MFP until they undergo a charge-exchange or ionization collision. If the collision of a Frank–Condon atom is a charge-exchange, the atom takes on an average energy of the ions in that region.

IV. NEUTRAL PARTICLE RECYCLING CALCULATIONS

A. Geometric model

The analysis presented in this paper was performed on a 2D mesh generated by the 2D fluids code UEDGE and extended to the walls of the confinement vessel, as discussed in the previous section. The computational grid shown in Fig. 3 consists of a pedestal (PED) region extending inward from the separatrix for a distance sufficient to attenuate the neutral density by a couple of orders of magnitude [about 7% of the normalized radius (ρ)], a SOL region extending outward from the separatrix to the outer edge of the UEDGE computational grid, a halo (HALO) region extending from the exterior of the UEDGE computation grid to the material wall, inner and outer divertor (DIV) regions extending from the X-point to the divertor targets, and a PFR. Also shown in the figure is a CORE region, which is represented in the GTNEUT calculation as an albedo (fractional reflection) boundary condition for the inner surface of the PED region.

The lines going around the plasma in the poloidal direction in Fig. 3 are the flux surfaces produced from the EFIT. "Radial" lines crossing these flux surfaces extend inward from the separatrix across the PED region to the CORE region (at $\rho<0.93$) and outward from the separatrix across the SOL to the outer edge of the UEDGE computational grid, and then across the surrounding HALO region to the material wall. The regions formed by these intersecting "poloidal" and radial lines define the computation grid for the GTNEUT calculation. Neutral densities, ionization rates, etc. are calculated in the grid regions formed by the intersection of these radial and poloidal surfaces. Each of these grid regions can be identified by a radial location associated with the bounding flux surfaces and a poloidal location defined by where its bounding radial lines intersect the separatrix (this poloidal distance along the separatrix is measured in the clockwise direction with respect to an origin where the separatrix intersects the target plate in the inner divertor). For example, a poloidal distribution of ionization rates at $\rho=0.96$ in the pedestal would be constructed by plotting the ionization rate

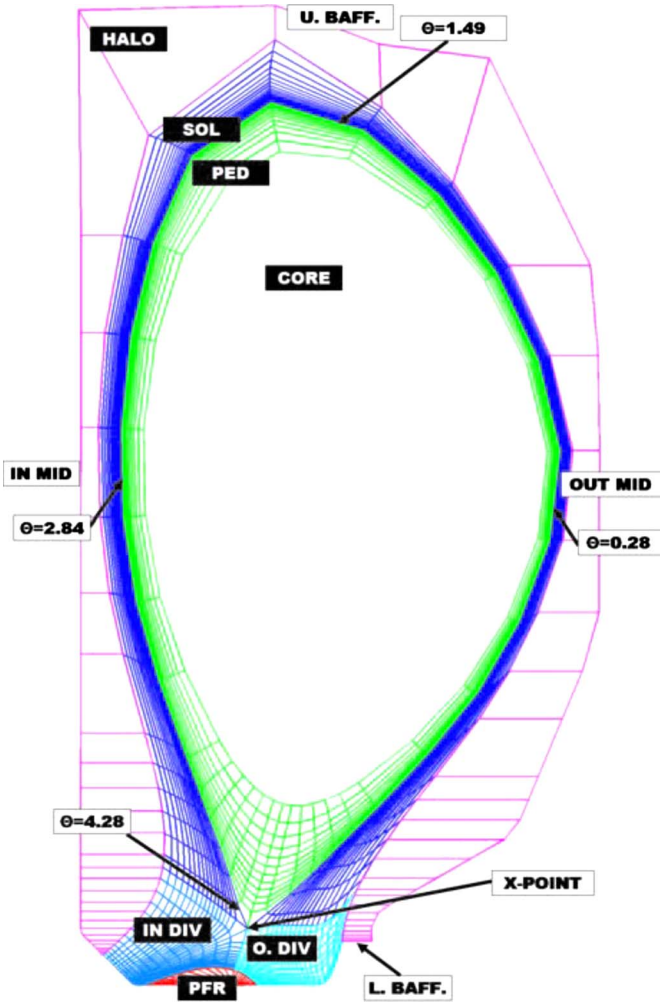

FIG. 3. (Color online) 2D geometric model used in GTNEUT analysis.

in each grid region between the flux surfaces bounding $\rho=0.96$ versus the poloidal location at which the radial lines bounding the grid region intersected the separatrix. The poloidal distribution of the total ionization in the pedestal would then be plotted by summing the ionization over all cells in the pedestal bounded by two radial lines intersecting the separatrix at a given poloidal distance along the separatrix.

The background plasma parameters in the upper PED, outboard PED, and SOL were taken from the Thomson scattering data and used to benchmark the UEDGE calculation of the background plasma parameters throughout the PED, SOL, and DIV regions.[16] The HALO region was assumed to have a uniform temperature and density distribution (ne,ni=0.13e19 #/m^3 and Te,Ti=12 eV). The PFR is assumed to have a uniform temperature and density (ne,ni=1e18 #/m^3 and Te,Ti=3 eV). The plasma CORE is not included in the GTNEUT calculation, but the net number of neutrals crossing the boundary from the PED to the CORE is considered to be ionized in the core.

Several points of interest are also illustrated in Fig. 3. The lower and upper baffle locations (L. BAFF. and U. BAFF.) are where the recycling calculated by the window frame method and shown in Table I is assumed to take place.

TABLE I. Neutral sources from recycling ions obtained from surface mounted probes (divertor) and window frame analysis (baffles).

	Ion recycling sources (#/s)
Upper baffle	$8.13\times10^{+20}$
Lower baffle	$8.13\times10^{+20}$
Inner divertor	$5.55\times10^{+21}$
Outer divertor	$6.04\times10^{+21}$

In order to discuss the poloidal distribution of neutral particles and reaction rates, it is convenient to define certain poloidal reference points. It is easiest to do this in terms of an angle θ. Starting at the OUTMID, $\theta=0$. If we consider the separatrix in the 2D calculation model as a one-dimensional (1D) strip starting at $\theta=0$, the midpoint of the first computation cell occurs at $\theta=0.28$. Thus, $\theta=0.28$ is the OUTMID reference point. Continuing along the 1D strip (separatrix) in the counterclockwise direction, the next reference point is the cell along the separatrix located at the upper baffle (U. BAFF.) location ($\theta=1.49$). The next reference point is the inner midplane location at $\theta=2.84$. Finally, the last reference point is at the X-point. There are two sides of the X-point, an inboard and an outboard side. For our figures showing the poloidal distributions, the SOL always starts at the inboard side of the X-point ($\theta=4.28$) and continues in a clockwise fashion around the separatrix back to the outboard side of the X-point. The divertor regions are represented as short extensions on both ends of the SOL.

B. Overall particle balance

The overall ion particle balance on the region inside the separatrix (CORE+PED) is shown in Table II for both sets of background plasma parameters. If the UEDGE solution for the background plasma parameters and the GTNEUT solution for the neutral particle ionization rates were self-consistent and if the Porter method[23] for determining the experimental ion outflow across the separatrix was precise, then the experimental outflow of ions across the separatrix should be balanced at steady-state by the neutral beam ion source plus the ionization of recycling neutrals in the CORE+PED regions. As shown in Table II, there is a significant discrepancy between the sources of ions in the core (due to neutral beams and to the calculated neutral inflow across the separatrix) and the experimental ion outflow across the separatrix determined by the Porter method.[23] This discrepancy is larger than the quoted $\pm30\%$ uncertainty in the determination of the experimental ion outflow associated with uncertainty in the experimental data.[23] However, as discussed at the end of Sec. II, there are other unquantified uncertainties in the determination of the experimental ion outflow across the separatrix.

As indicated by the last line in Table II, the use of the detached UEDGE background plasma parameters (with the larger recombination neutral source) results in significantly better agreement between the ion sources and losses. In both cases the difference between ion sources and losses are larger than the estimated[23] 30% error in the determination of the

TABLE II. Ion global particle balance on CORE+PED.

	Attached	Detached	Determined
Loss—ion outflow across separatrix (#/s)[a]	$\mathbf{2.74\times10^{+21}}$	$\mathbf{2.74\times10^{+21}}$	Experiment
Sources			
Neutral beam ion source (#/s)	$0.386\times10^{+21}$	$0.386\times10^{+21}$	Known
Ionization of recycling neutrals (#/s)	$0.927\times10^{+21}$	$1.313\times10^{+21}$	GTNEUT[b]
Total ion source (#/s)	$\mathbf{1.316\times10^{+21}}$	$\mathbf{1.699\times10^{+21}}$	
Ion (outflow–sources) (#/s)	$\mathbf{1.424\times10^{+21}}$	$\mathbf{1.041\times10^{+21}}$	

[a]Determine experimentally using the Porter method (Ref. 23).
[b]See Refs. 18 and 26–28 for comparison of GTNEUT with Monte Carlo and experiment.

ion outflow across the separatrix. This result is consistent with the earlier conclusion[16] that the plasma is probably detached at the inner divertor in this shot.

The overall neutral particle balance between sources (ion recycling and recombination) and sinks is shown in Table III for both the attached and detached background plasma parameters. The distribution of neutral particle ionization rates among the various regions is also given in Table III. Clearly, the majority of the ionization (≈70%) takes place in the divertors, and only 7% of the recycling and recombined neutrals actually make it across the separatrix to fuel the pedestal and core. The percentage of the total neutral ionization that is in each region and the percentage of the total neutral source from recycling and from recombination are given in parentheses in Table III.

C. Neutral particle fluxes recycling from wall surface and crossing separatrix

With reference to the poloidal locations identified in Fig. 3, the neutral particle fluxes recycling from the wall are shown in Fig. 4. Two types of recycling neutral particle fluxes are shown—those produced by the recycling of the experimental incident ion fluxes (which are inputs to the GTNEUT calculation) and those produced by the recycling of the calculated (GTNEUT) incident neutral fluxes. The incident ion fluxes measured by the probes at the divertor targets of course recycle as neutrals from those locations, but the incident ion fluxes determined from probe measurements on the outboard using the window frame technique are represented in the GTNEUT calculation as being localized at the upper and lower baffles and are shown as single points in Fig. 4. The recycling neutral fluxes from incident ions are consistent with the measured ion fluxes to the wall—largest near the divertors but with a significant peaking at the upper and lower baffles.

These neutral fluxes from the wall resulting directly from the incident ion fluxes then charge-exchange somewhere in the edge plasma and produce neutral fluxes incident on the wall, which in turn recycle as neutral fluxes, charge-exchange, and produce neutral fluxes to the wall, etc. The sum total of the recycling neutral fluxes from the wall due to charge-exchange (and elastic scatter) incident neutral fluxes on the walls is also shown in Fig. 4, for the GTNEUT calculations using both the attached and detached background plasma parameters. The recycling fluxes produced by the recycling incident charge-exchange neutral fluxes dominate the recycling fluxes produced by incident ion fluxes. The poloidal length along the chamber wall is measured clockwise from the point on the chamber wall in the lower left of Fig. 3 where the inner divertor and halo regions meet.

The recombination source is calculated in all regions but is only significant in the inner divertor region. As shown in Table III, the recombination source is only 1% of the total

TABLE III. Global neutral particle balance on entire computation domain.

	Attached	Detached	Determined
Ionization (sinks) (#/s)			
CORE	$0.129\times10^{+21}$ (1%)	$0.193\times10^{+21}$ (1%)	GTNEUT
PED	$0.798\times10^{+21}$ (6%)	$1.120\times10^{+21}$ (6%)	
SOL	$1.910\times10^{+21}$ (15%)	$2.670\times10^{+21}$ (14%)	
HALO	$1.120\times10^{+21}$ (9%)	$2.020\times10^{+21}$ (11%)	
IN DIV	$4.380\times10^{+21}$ (33%)	$7.390\times10^{+21}$ (39%)	
OUT DIV	$4.770\times10^{+21}$ (36%)	$5.430\times10^{+21}$ (29%)	
PFR	$0.107\times10^{+19}$ (≪1%)	$0.365\times10^{+19}$ (≪1%)	
Total ionization	$\mathbf{13.108\times10^{+21}}$	$\mathbf{18.827\times10^{+21}}$	
Sources (#/s)			
Ion recycling	$13.217\times10^{+21}$ (99%)	$13.217\times10^{+21}$ (66%)	Experiment
Recombination	$0.147\times10^{+21}$ (1%)	$6.243\times10^{+21}$ (34%)	UEDGE
Total sources	$\mathbf{13.364\times10^{+21}}$	$\mathbf{19.460\times10^{+21}}$	

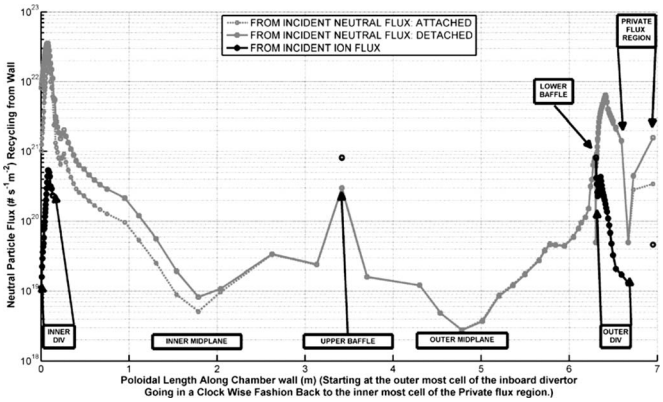

FIG. 4. Poloidal distribution of neutral fluxes recycling from the wall.

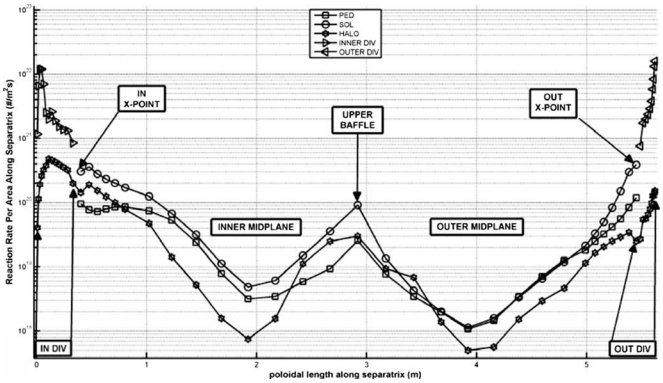

FIG. 6. Poloidal distribution of ionization rates per unit area along the separatrix (detached).

neutral source for the attached background plasma but is 34% of the neutral source for the detached background plasma.

The inward neutral fluxes across the separatrix are shown in Fig. 5. Both the partial inward flux and the net inward flux (when the outward flux of charge-exchanged and scattered neutrals is subtracted) across the separatrix are shown. The inward partial flux is directly related to the recycling source, while the net inward flux is the quantity relevant to particle balance inside the separatrix. The plasma is fueled primarily through the X-point region by neutrals recycling from the divertor targets or recombining in the inner divertor region. There is a strong secondary fueling due to ions recycling at the upper and lower baffles.

D. Poloidal distributions of ionization and charge-exchange rates

A neutral particle recycling from the wall or formed by recombination will ultimately be ionized. It is of interest to examine in which region this ionization will take place. The "radially summed" ionization rate in the various regions defined in Fig. 3 is plotted as a function of poloidal location along the separatrix in Figs. 6 and 7.

With reference to Fig. 3, the computational grid is constructed so that for each segment along the separatrix, there is a corresponding set of SOL regions extending outward, beyond which is a HALO region, and a corresponding set of PED regions extending inwards. In the previous Monte Carlo (DEGAS2) calculations[16] of this discharge, the total ionization in all the PED regions "behind" a given segment along the separatrix was summed and divided by the surface area of that separatrix segment (the segment length extended toroidally around the plasma chamber) in order to obtain a proxy for the poloidal distribution of the radial neutral particle flux crossing the separatrix (the statistical nature of the Monte Carlo solution leads to a rather erratic direct calculation of this quantity). In order to touch base with these Monte Carlo calculations, this same quantity calculated with GTNEUT is plotted in Fig. 6 as the PED ionization (with units of flux) for the detached plasma background case. Similar quantities constructed from the ionization in the corresponding HALO region and summed "radially" over the corresponding SOL regions are also plotted. The computation grid extends almost perpendicular to the separatrix in the two divertor regions, and the summed ionization rates over the regions corresponding to a given segment along the separatrix (divided by the area of that segment extended toroidally) are plotted as the INNER DIV and OUTER DIV ionization in Fig. 6. The main difference between the ionization rates shown in Fig. 6 for the detached case and those calculated with the attached background plasma parameters is a factor of 2 lower ionization rates in the HALO, SOL, and PED ionization vi-

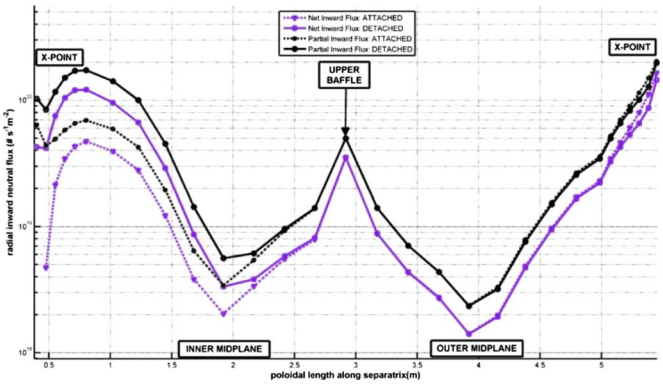

FIG. 5. (Color online) Inward partial (in) and net (in minus out) neutral fluxes across the separatrix.

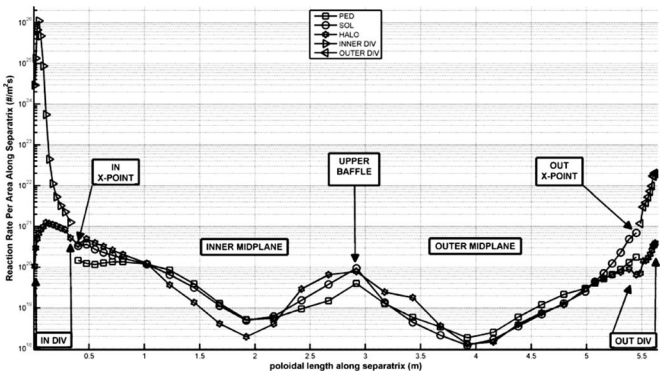

FIG. 7. Poloidal distribution of charge-exchange rates per unit area along the separatrix (detached).

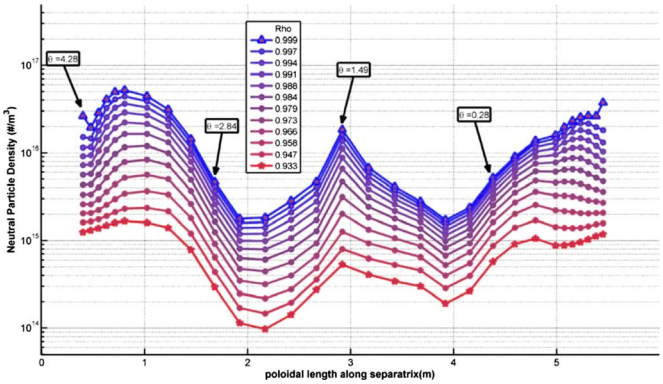

FIG. 8. (Color online) Poloidal distribution of neutral density over flux surface in edge pedestal (detached) (see Fig. 3 for locations corresponding to θs).

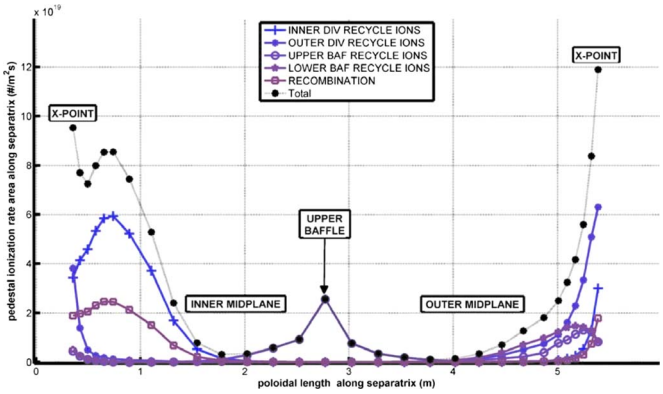

FIG. 10. (Color online) Poloidal distribution of PED ionization rate per unit area along separatrix due to each recycling source separately (detached).

cinity of the inner divertor due to the lower recombination source for the attached case.

The major part of the ionization (≈70%) takes place in the divertor and, to a lesser extent, in the SOL (≈15%). The poloidal distribution of ionization roughly corresponds to the poloidal distribution of the recycling sources shown in Fig. 4 and the location of a strong recombination source in the inner divertor for the detached background plasma parameters. The reduction in the inner divertor ionization rate just in front of the target, where the temperature is about 1 eV, is notable in Fig. 6 for the detached background plasma parameters.

Charge-exchange reaction rates, constructed in the same manner as discussed above for ionization, are shown in Fig. 7 for the detached plasma background. The poloidal distribution roughly corresponds to the poloidal distribution of the wall recycling neutral fluxes and recombination source in the inner divertor. The charge-exchange rates are generally comparable to or larger than the ionization rates; the enormous charge-exchange rate in the inner divertor for the detached background plasma is notable. For the attached background plasma, the large peaking of the charge-exchange rate in the inner divertor is reduced by several orders of magnitude, and the charge-exchange rates in the HALO, SOL, and PED in the vicinity of the inner divertor are reduced by a factor of 2.

E. Neutral penetration of the edge pedestal

The poloidal distribution over the flux surface of the neutral atom density is plotted for several values of the normalized radius (ρ) in Fig. 8 for the detached plasma background case. For the attached plasma background, the ionization rates were a factor of 2 lower in the vicinity of the inner divertor because of the lower recombination source. Similar distributions were calculated for the ionization and recombination rates.

It is clear that there are orders of magnitude variations in the neutral atom density, the ionization fueling source, the electron ionization cooling, and the ion charge-exchange cooling over the flux surface in the plasma edge pedestal. This raises questions about the adequacy of 1D ion particle and energy transport calculations that are frequently made (e.g., Ref. 10) in the edge pedestal region in the presence of strong neutral recycling. For example, the more than two orders of magnitude difference between the ionization rate in the pedestal just above and to the left of the X-point (poloidal length of ≈1) and the upper inboard quadrant (poloidal length of ≈2) causes a similar variation in the ionization particle source and electron cooling rate, which could drive edge thermal instabilities (e.g., MARFEs) that might not be predicted by a 1D radial calculation in which the poloidal variations were averaged out.

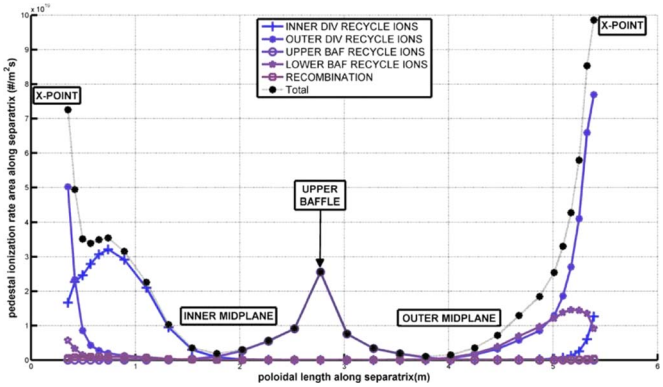

FIG. 9. (Color online) Poloidal distribution of PED ionization rate per unit area along the separatrix due to each recycling source separately (attached).

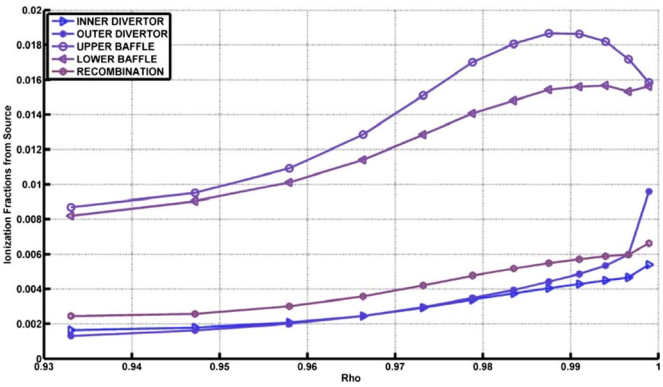

FIG. 11. (Color online) Effectiveness of neutrals from different sources in fueling the pedestal (fraction of source neutrals ionized on each flux surface in pedestal) (attached).

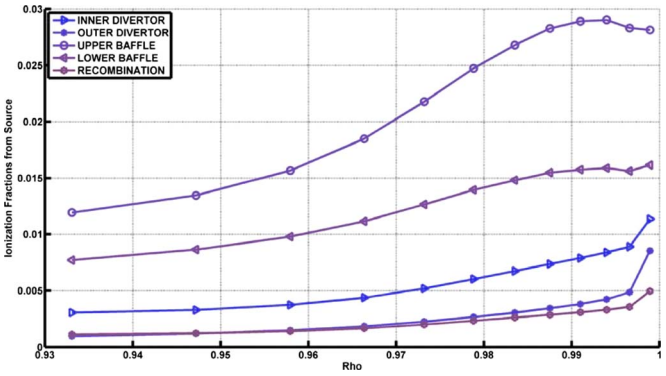

FIG. 12. (Color online) Effectiveness of neutrals from different sources in fueling the pedestal (fraction of source neutrals ionized on each flux surface in pedestal) (detached).

F. Importance of different neutral particle sources in fueling pedestal and core

The importance of a given neutral particle source (e.g., upper baffle recycling or inner divertor recombination) for fueling the pedestal and core depends on two factors—the strength of the source and the fraction of the particles from a given source that are transported inward across the separatrix. The poloidal distribution of the PED ionization rates (constructed by radially summing the ionization occurring in the PED regions inboard of a given segment along the separatrix and dividing by the area of that segment extended toroidally around the plasma, as previously described) resulting from each individual neutral particle source are shown for the attached and detached background plasmas in Figs. 9 and 10. Not surprisingly, the inner and outer divertor ion recycling sources are most important for fueling the region around the X-point for the attached background plasma, and the upper baffle recycling ion source is most important for fueling the top of the plasma near the upper baffle. For the detached background plasma, the recombination source (mostly in the inner divertor) is also an important contributor to the X-point fueling of the pedestal.

In order to characterize the likelihood that a neutral particle from a given source would be transported across the separatrix and cause a fueling (ionization) event on a given flux surface (ρ) in the pedestal, we first calculated ionization rates as a function of ρ and θ, such as those shown in Fig. 8, for each source. We then summed these plots poloidally to obtain the total ionization rate on each flux surface due to each source, then divided by the respective source strengths to obtain the fraction of neutrals from a given source that would cross the separatrix to refuel the pedestal on a given flux surface. This "fraction" is plotted versus flux surfaces (ρ) in Figs. 11 and 12 for the attached and detached background plasma parameters, respectively. Neutrals recycling from the upper and lower baffles are more effective at penetrating across the separatrix to fuel the pedestal than neutrals recycling or recombining in the divertor. This is understandable because of the shorter distance (in MFP) the neutrals must travel from the baffle to separatrix than from the divertor plates to the separatrix.

Neutrals recycling from the inner divertor are more effective in fueling the pedestal than neutrals recycling from the outer divertor for the detached case in which the ionization MFP in the cold inner divertor become longer.

Summing the ionization rate due to each source over the entire pedestal and core regions (basically integrating the pedestal integration in Figs. 11 and 12 over the radial extent of the pedestal) and then dividing by the strength of that source yield the fraction of the neutrals produced by each source that crosses the separatrix to fuel (ionize in) the confined plasma shown in Table IV.

It must be emphasized that although individual neutrals recycling from the baffles have a better chance of fueling the pedestal than do individual neutrals recycling from the divertor, the greater number of neutrals recycling or recombining in the divertor than recycling from the baffles results in the divertor being the principal source of neutrals refueling in this discharge, as shown in Figs. 13 and 14, which were obtained by multiplying the curves in Figs. 11 and 12 by the respective source strengths given in Table I and recombination strengths given in Table III. These figures also show how the relative contributions of the various neutral sources to fueling the pedestal depend on the background plasma parameters (note that only the recombination neutral source calculated with UEDGE is different for the GTNEUT calculations with the attached and detached plasma backgrounds since the ion recycling neutral sources are taken from experiment and are independent of the background plasma parameters).

TABLE IV. Fraction of neutrals from each source ionized in PED+CORE.

	Fraction					
	Attached			Detached		
Case	PED (%)	CORE (%)	PED+CORE (%)	PED (%)	CORE (%)	PED+CORE (%)
Upper baffle recycling	17.5	4.0	**21.50**	27.6	5.4	**33.00**
Lower baffle recycling	15.2	3.7	**18.90**	15.8	3.6	**19.40**
Inner divertor recycling	4.0	0.7	**4.70**	7.6	1.5	**9.10**
Outer divertor recycling	4.7	0.4	**5.10**	3.8	0.3	**4.10**
Recombination	2.4	1.3	**3.70**	3.0	0.5	**3.50**

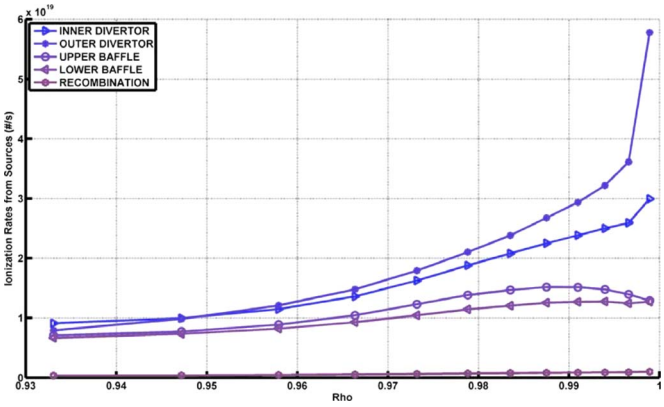

FIG. 13. (Color online) Ionization fueling rates in the pedestal from different sources (attached).

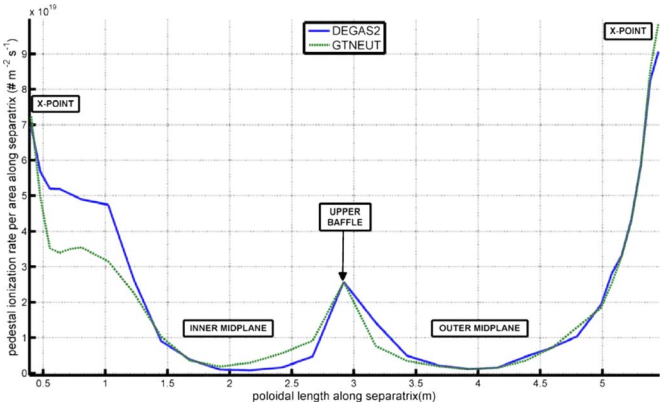

FIG. 15. (Color online) Poloidal distributions of PED+CORE ionization rate per unit separatrix area calculated by GTNEUT and DEGAS2 (attached).

G. Computational and experimental uncertainty

There is a fair amount of uncertainty in the analysis we have presented. As previously mentioned, the accuracy of the experimental determination of the ion outflow from the CORE+PED across the separatrix into the SOL, due to uncertainty in the experimental data, is judged to be about ±30%,[23] but experimental uncertainties are not the only ones.

A measure of the computational uncertainty in the GTNEUT solution is obtained by performing an internal particle balance on the input sources minus the calculated sinks. The difference is a measure of the overall error in the calculation, and local errors could be greater or less. For the attached background plasma, this error was about 1.8%, and for the detached background plasma, it was about 3.2%. While GTNEUT has been extensively benchmarked against Monte Carlo calculations,[26–28,18] it has not previously been used for problems with so many (1560) regions, some of which have MFPs in the tens of meters. The error in the internal particle balance may be due to errors in inverting such a large, albeit sparse, matrix. Additionally, some errors may be occurring in the evaluation of the transmission coefficients. There is some evidence[31] that the approximate evaluation of the Bickley functions used in the angular integration to obtain the transmission coefficients may be a source of error.

A Monte Carlo neutrals calculation for this same shot, using the same two sets of background plasma parameters, has been performed[13] with DEGAS2.[19] The 2D mesh was identical except in the halo regions, where a different grid structure from that shown in Fig. 3 was used to extend the UEDGE mesh to the wall of the confinement vessel in the DEGAS2 calculation. With 10 000 histories each for the four wall recycling sources and for the recombination source, the overall statistical uncertainty in the DEGAS2 calculation is estimated to be roughly ±5%, but the statistical uncertainty in the calculation of ionization rates in individual small regions could be significantly larger.

The radially integrated PED+CORE ionization rates, determined as discussed above, calculated with GTNEUT and DEGAS2 are compared in Figs. 15 and 16. It is clear that the two calculations agree rather well except in the region on the inboard side just above the X-point. Possible causes of this disagreement are discussed below.

The GTNEUT and DEGAS2 calculations of the total ionization rate in the PED+CORE region are compared in Table V. Also shown are the overall particle balance error from Table III in the GTNEUT calculation, which is a measure of the global calculational uncertainty in GTNEUT, and the estimated statistical uncertainty in the DEGAS2 calculation of the ionization in the PED+CORE region.

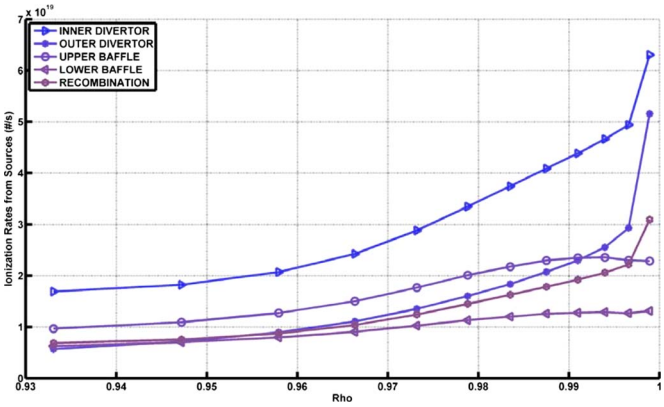

FIG. 14. (Color online) Ionization fueling rates in the pedestal from different sources (detached).

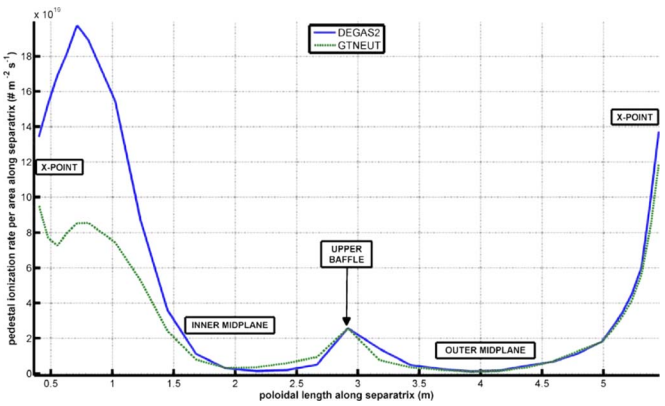

FIG. 16. (Color online) Poloidal distributions of PED+CORE ionization rate per unit separatrix area calculated by GTNEUT and DEGAS2 (detached).

TABLE V. Comparison of ionization rates in the PED+CORE calculated by GTNEUT and DEGAS2.

	GTNEUT		DEGAS2	
	Attached	Detached	Attached	Detached
Source strength (#/s)	$1.34\times10^{+22}$	$1.96\times10^{+22}$	$1.34\times10^{+22}$	$1.96\times10^{+22}$
Ionization rate (#/s) PED+CORE	$0.927\times10^{+21}$	$1.313\times10^{+21}$	$0.860\times10^{+21}$	$1.77\times10^{+21}$
Percent of source neutrals ionized in PED+CORE (%)	6.9	6.7	6.4	9.0
Calculation uncertainty (%)	1.8	3.2	5	5

Calculations of pedestal fueling for the two codes agree reasonably well for the attached background plasma parameters but differ more significantly for the detached background plasma parameters. Figure 16 indicates that most of this disagreement arises from differences in neutral transport just above the X-point on the inboard side. For the attached background plasma parameters, the disagreement between the two calculations is within the calculational uncertainty in the calculations. However, for the detached background plasma calculations, the disagreement would seem to be significantly larger than the calculational uncertainty, suggesting a discrepancy due to methods or data.

We conjecture that this discrepancy may be due to the different ways in which the two codes handle molecular transport. DEGAS2 fully models molecular transport with different species in the plasma edge. In GTNEUT molecules recycled from the wall are assumed to dissociate into Franck–Condon energy atoms in the first grid region in front of the wall and be transported with a MFP corresponding to that energy until they have a collision. The regions that would be most affected by the different treatments of molecular transport would be the regions with very low temperature (e.g., the inner divertor regions with the detached background plasma parameters). This conjecture is supported by a previous comparison[26] of GTNEUT and DEGAS for a different DIII-D shot, in which differences between calculated ionization rates between the two codes were reduced dramatically when the molecular transport calculation was turned off in the DEGAS calculation.

Other possible causes of this discrepancy could arise from differences in atomic physics data used by the two codes (which we believe based on previous work to be small) and to the treatment of a plasma flow dependence of the direction of charge-exchanged neutrals in DEGAS2, which is not available in GTNEUT.

V. SUGGESTED IMPROVEMENTS TO GTNEUT

The TEP methodology results in a large matrix equation relating the two partial fluxes across each interface in the computational domain indicated in Fig. 3, which is solved using a standard sparse matrix routine. In previous applications to problems with many fewer interfaces, the solution procedure went smoothly. However, with this large number of interfaces, we did encounter some difficulty (which we attributed to round-off error) in obtaining a solution in some cases. For problems of this size and larger, it would be good to implement a better sparse matrix routine.

The differences between the GTNEUT and DEGAS2 calculations near the inner divertor shown in Figs. 15 and 16 are conjectured to be due to the differences in the treatment of molecules. As discussed at the end of Sec. IV, DEGAS2 explicitly accounts for molecular transport, whereas in GTNEUT the molecules are assumed to be dissociated in the region immediately adjacent to the wall and into atoms. The inclusion of molecular transport in GTNEUT would seem to be suggested.

We mention also two improvements suggested by a previous investigator[31] but not yet implemented. The method of angular integration used to find the transmission coefficients should be modified. The current routines take up approximately 85% of the computational time for a GTNEUT calculation. Additionally, there is reason to believe these routines could be responsible for round-off errors in the calculations.

VI. SUMMARY AND CONCLUSIONS

We have investigated in detail the neutral particle recycling and pedestal fueling from wall reflection and volumetric recombination sources in a DIII-D H-mode discharge. The investigation confirms previous studies[13,16] that the edge pedestal in DIII-D is primarily fueled by recycling and recombination neutrals from the divertor region.

We find that the penetration of recycling neutrals into the pedestal region is highly nonuniform poloidally both because the recycling and recombination sources are poloidally nonuniform and because neutral particles recycling from the upper baffle penetrate deeper into the pedestal (because the path length in MFPs is shorter) than neutrals recycling from the divertor region. Although the effects of poloidally asymmetric particle source and heat sinks will be ameliorated to some extent by rapid poloidal transport along the field lines, this result raises questions about the adequacy of 1D plasma transport calculations that are sometime employed in the edge pedestal and suggests an area of further investigation.

Finally, a comparison of DEGAS2 and GTNEUT calculations of neutral ionization rates indicates relatively good agreement between the two codes except in the immediate vicinity of the inner divertor, where the differences in treatment of molecular transport are thought to be responsible for the significant discrepancy in predicted neutral influxes across the separatrix.

ACKNOWLEDGMENTS

The support provided by R. J. Groebner of General Atomics in the original suggestion of this line of research and his detailed review of this paper and by T. D. Rognlien of Lawrence Livermore National Laboratory in the adaptation of the UEDGE geometric grid generator for constructing GTNEUT geometry input are gratefully acknowledged. Extensive suggestions for clarification by the reviewer are gratefully acknowledged. This work was supported by the U.S. Dept. of Energy under Grant No. DE-FG02-ER54538 with the Georgia Tech Research Corporation, Contract No. DE-AC03-99ER54463 with General Atomics Co., and Contract No. DE-AC52-07NA27344 with the University of California.

[1] A. Niemczewski, I. H. Hutchinson, B. LaBombard, B. Lipschultz, and G. M. McCracken, Nucl. Fusion **37**, 151 (1997).
[2] R. J. Colchin, R. Maingi, M. E. Fenstermacher, T. N. Carlson, R. C. Isler, L. W. Owen, and R. J. Groebner, Nucl. Fusion **40**, 175 (2000).
[3] W. M. Stacey, M. A. Mahdavi, R. Maingi, and T. W. Petrie, Phys. Plasmas **6**, 179 (1999).
[4] M. Z. Tokar, J. Rapp, D. Reiser, U. Samm, G. C. Schuller, G. Sergienko, and P. J. de Vries, J. Nucl. Mater. **266–269**, 958 (1999).
[5] K. Tsuchiya, H. Takenaga, T. Fukuda, Y. Kamada, S. Ishida, M. Sato, T. Takizuka, and JT-60 Team, Plasma Phys. Controlled Fusion, **38**, 1295 (1996).
[6] R. J. Groebner, M. A. Mahdavi, A. W. Leonard, T. H. Osborne, and G. D. Porter, Phys. Plasmas **9**, 2134 (2002).
[7] W. M. Stacey, Z. W. Friis, T. W. Petrie, and A. W. Leonard, Phys. Plasmas **12**, 072518 (2005).
[8] M. A. Mahdavi, R. Maingi, R. J. Groebner, A. W. Leonard, T. H. Osborne, and G. D. Porter, Phys. Plasmas **10**, 3984 (2003).
[9] W. M. Stacey and R. J. Groebner, Phys. Plasmas **10**, 2412 (2003).
[10] W. M. Stacey and R. J. Groebner, Phys. Plasmas **13**, 072510 (2006).
[11] M. Groth, L. W. Owen, G. D. Porter, N. H. Brooks, M. E. Fenstermacher, W. H. Meyer, A. W. Leonard, T. W. Petrie, D. L. Rudakov, G. Wang, J. G. Watkins, and N. S. Wolf, J. Nucl. Mater. **337–339**, 425 (2005).
[12] M. E. Rensink, M. Groth, G. D. Porter, T. D. Rognlien, D. L. Rudakov, and J. G. Watkins, J. Nucl. Mater. **363–365**, 816 (2007).
[13] A. W. Leonard, J. A. Boedo, M. Groth, B. L. Lipschultz, G. D. Porter, D. L. Rudakov, and D. G. Whyte, J. Nucl. Mater. **363–365**, 1066 (2007).
[14] D. G. Whyte, B. L. Lipschultz, P. C. Stangeby, J. Boedo, D. L. Rudakov, J. G. Watkins, and W. P. West, Plasma Phys. Controlled Fusion **47**, 1579 (2005).
[15] B. I. Lipschultz, D. G. Whyte, and B. LaBombard, Plasma Phys. Controlled Fusion **47**, 1559 (2005).
[16] A. W. Leonard, M. Groth, G. D. Porter, and M. E. Rensink, J. Nucl. Mater. **390–391**, 470 (2009).
[17] J. Mandrekas, Comput. Phys. Commun. **161**, 36 (2004).
[18] D.-K. Zhang, J. Mandrekas, and W. M. Stacey, Phys. Plasmas **13**, 062509 (2006).
[19] D. Stotler, C. Karney, R. Kanzleiter, and S. Jaishankar, User's Guide for DEGAS2 CVS, Revision: 1.4, http://w3.pppl.gov/degas2/Doc/degas2_all.pdf (2007).
[20] D. Reiter, "The EIRENE Code user's manual," Julich KFA Report, 2005.
[21] J. D. Callen, R. J. Groebner, T. H. Osborne, J. M. Canik, L. W. Owen, A. Y. Pankin, T. Rafiq, T. D. Rognlien, and W. M. Stacey, "Analysis of pedestal transport," Nucl. Fusion (submitted).
[22] T. Rognlien, Users Manual for the UEDGE Edge-Plasma Transport Code, 2000, available from https://e-reports-ext.llnl.gov/pdf/246621.pdf.
[23] G. D. Porter and DIII-D Team, Phys. Plasmas, **5**, 4311 (1998).
[24] W. M. Stacey and J. Mandrekas, Nucl. Fusion **34**, 1385 (1994).
[25] W. M. Stacey, Phys. Plasmas **4**, 179 (1997).
[26] J. Mandrekas, R. J. Colchin, W. M. Stacey, D. Zhang, and L. W. Owen, Nucl. Fusion **43**, 314 (2003).
[27] R. Rubilar, W. M. Stacey, and J. Mandrekas, Nucl. Fusion **41**, 1003 (2001).
[28] W. M. Stacey, J. Mandrekas, and W. M. Stacey, Fusion Sci. Technol. **40**, 66 (2001).
[29] L. L. Lao, Nucl. Fusion **30**, 1035 (1990).
[30] Z. W. Friis, "A semi-automated procedure for creating geometry and background plasma input files for the GTNEUT 2D neutral particle transport code using the UEDGE plasma edge," Georgia Tech Report, 2009, available from www.frc.gatech.edu on Neutrals Transport page.
[31] D. Zhang, "Neutral particle transport in plasma edge using transmission escape probability (TEP) method," Ph.D. thesis, Georgia Institute of Technology, 2005.